Journal of Organometallic Chemistry, *447* (1993) 241–249

JOM 23198

^{13}C and ^{19}F NMR study on the structure and conformation of tricarbonylchromium complexes of biphenyl derivatives

Przemysław Szczeciński and Janusz Zachara

Department of Chemistry, Warsaw University of Technology, Noakowskiego 3, 00-664 Warszawa (Poland)

(Received July 29, 1992)

Abstract

The ^{13}C and ^{19}F NMR spectra of 2,2′-difluoro-4,4′-dimethylbiphenyl (BIP), 4,5-difluoro-9,10-dihydrophenanthrene (PHE) and their tricarbonylchromium complexes are reported. The ^{13}C–^{19}F couplings between carbonyl carbons and aromatic fluorine were used to determine the structure and conformation of the investigated complexes. To support the conclusions obtained, the structure of one of the BIP complexes was established by X-ray crystallography.

1. Introduction

In our previous papers [1–3] the coupling between carbonyl carbons and aromatic fluorine in (η^6-fluoroarene)tricarbonylchromium complexes has been reported. On the basis of the data for *meta* and *para* substituted fluorobenzene complexes we have established that the ^{13}C–^{19}F coupling constant depends on the ability of the ring substituent to contribute to the stabilization of the rotamer A (see Fig. 1), in which C_{Ar}–F and Cr–CO bonds are in *eclipsed* conformation [1]. Also in chelate (η^6-fluorobenzyl)diphenylphosphitodicarbonylchromiums, in which the relative conformation of the carbonyl groups and aromatic substituents is fixed, the coupling has been observed only for carbonyl carbons located sufficiently close to the aromatic fluorine [2]. Those facts led us to the conclusion that the nuclear spin information is probably mainly transmitted between coupled nuclei "through-space". If this is true the observed coupling constant, reflecting the distance between the nuclei involved, might serve as a direct probe in the investigations of the conformation of the carbonylchromium complexes. To our knowledge all "through-space" C–F couplings reported in the literature result primarily from the overlap of fluorine lone electron pair and sterically opposed C–H bond orbitals [4–7]. As discussed here, coupling must involve a different way of transmission of spin information. We believe it arises from the direct interaction of the p orbital of fluorine and the π (or π^*) orbital of the CO triple bond. In all compounds hitherto investigated, fluorine was attached to the complexed arene ring. Thus, the coupled nuclei were separated by three bonds only and "through-bond" spin–spin interaction could not be definitely ruled out. We were interested to know if the carbonyl carbon–fluorine coupling is observed when more bonds separate those nuclei but when they are still located close to each other. Biphenyl derivatives seemed to meet the above demands. Here we report the results obtained for the following complexes (see Fig. 2): (±)-(R^*,R^*)[(1,2,3,4,5,6-η)-2,2′-difluoro-6,6′-dimethylbiphenyl]tricarbonylchromium (**1**), (±)-(R^*,S^*)-[(1,2,3,4,5,6-η)-2,2′-difluoro-6,6′-dimethylbiphenyl]tricarbonyl, chromium (**2**), (±)-[(1,2,3,4,4*a*,10*a*-η)-4,5-difluoro-9,10-dihydrophenanthrene]tricarbonylchromium (**3**) and (±)-(S^*,S^*)-[(1,2,3,4,4*a*,10a-η)(4*b*,5,6,7,8,8*a*-η)-4,5-difluoro-9,10-dihydrophenanthrene]bis(tricarbonylchromium) (**4**).

2. Experimental section

BIP [8] and PHE [9] were prepared using literature methods. Complexes were obtained by reaction of ligand with $Cr(CO)_6$ in Bu_2OH/THF (10/1) mixture [10]. Compounds **1–4** were separated by column chro-

---

Correspondence to: Dr. P. Szczeciński.

0022-328X/93/$6.00

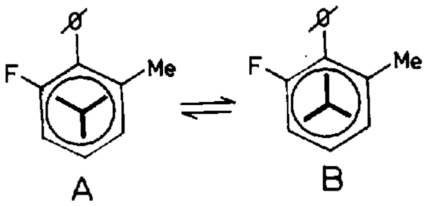

Fig. 1. Equilibrium between rotamers **A** and **B** of $Cr(CO)_3$ tripod in arenetricarbonylchromium complexes.

matography on silica gel (Merck-60; 0.063–0.2) using 5% Et_2O/hexane as eluent. Their melting points were 170–173°C, 126–129°C, 143–145°C and 173°(dec.), respectively.

^{13}C NMR of [η^6-3-(trifluoromethyl)anisole]tricarbonylchromium (m.p. 48–50°) in $CDCl_3$ (ppm; J(C–F) in parentheses in Hz): 55.16 (q, CH_3, 2.1), 73.43 (q, C2, 2.6), 78.19 (s, C6), 81.89 (q, C4, 2.7), 92.08 (s, C5), 99.52 (q, C3, 36.7), 123.59 (q, CF_3, 273.8), 141.10 (s, C1), 230.96 (s, CO).

^{13}C NMR of 2-fluoropyridinepentacarbonylchromium (m.p. 88–92°C dec.) in $CDCl_3$ (ppm, J(C–F) in parentheses in Hz): 111.83 (d, C3, 22.9), 121.27 (d, C5, 3.4), 142.71 (d, C4, 9.8), 153.57 (s, C6), 165.36 (d, C2, 254.4), 214.02 (d, *cis*-CO, 7.6), 221.85 (d, *trans*-CO, 1.7).

Solution of the complexes (*ca.* 0.5 M) in $CDCl_3$ were prepared under argon, degassed and sealed in 5

TABLE 1. ^{13}C chemical shifts (ppm) for the investigated compounds

Carbon	BIP	1	2		PHE	3	4
1		94.17	91.95	4*a*		89.08	84.75
2		144.60	145.05	4		143.31	143.66
3		76.15	74.88	3		78.33	78.14
4		93.54	92.95	2		91.32	91.62
5		86.34	85.98	1		87.63	86.86
6		110.43	109.30	10*a*		111.39	110.15
CH_3		19.15	18.91	CH_2		28.74	28.70
1′	122.08	116.95	117.13	4*b*	118.39	115.62	
2′	160.00	161.20	159.15	5	159.61	159.95	
3′	112.72	112.75	113.94	6	114.66	115.30	
4′	129.14	130.30	130.40	7	128.86	130.16	
5′	125.41	127.07	125.71	8	122.90	123.39	
6′	139.43	140.20	140.48	8*a*	141.67	141.05	
CH_3'	19.33	21.43	19.70	CH_2'	29.76	29.75	

TABLE 2. $^{13}C-^{19}F$ and $^{13}C-^{19}F'$ (in parentheses [a]) coupling constants for investigated compounds, in Hz

Compound	BIP			1	2		PHE	3	4
Carbon		J(F–F′)	$\Delta\delta_{F,F'}$ [c]			Carbon			
1				15.8(2.8)	15.9(0.5)	4*a*		13.6(1.6)	8.7 [g]
2				264.5(0.9)	262.7	4		272.2(0.5)	−275.6(1.1) [b,f]
3				22.6	21.8	3		22.8	23.6 [g]
4				8.2	8.0	2		7.9	7.8 [g]
5				0	0.5	1		0	0 [g]
6				3.8(1.5)	3.4	10*a*		4.6	3.6 [g]
CH_3				2.2(1.2)	1.2(0.8)	CH_2		1.1	unresolved
1′	17.3(1.1)	1.4	3.8	13.9(1.1)	13.8(0.8)	4*b*	13.0 [g]	13.6(3.4)	
2′	−244.1(0.6)	1.2	24.0	245.4(0.4)	248.7(0.4)	5	−254.4(1.6) [b,e]	256.1	
3′	22.6(0.2)	1.5	7.1	25.2	23.8	6	24.1 [g]	23.5	
4′	9.0(0.3)	1.4	2.0	9.8	9.2	7	9.6 [g]	9.3	
5′	2.8(0.1)	1.5	1.1	3.0	3.4	8	2.3 [g]	3.1	
6′	2.7(0.9)	1.2	1.7	1.1(0.4)	0.8(0.5)	8*a*	4.0 [g]	2.7	
CH_3'	3.7 [g]			2.8(1.4)	2.8(1.1)	CH_2'	2.1 [g]	2.4	

[a] Where value is not given this coupling is not observed.

[b] Data obtained from numerical analysis of ^{13}C NMR spectra.

[c] Differential isotope shift for ^{19}F caused by ^{13}C in Hz at 282 MHz.

[d] $\Delta\delta_{F,F'}$ assumed equal to 24 Hz and not fitted.

[e] $\Delta\delta_{F,F'} = 24.3$ Hz

[f] $\Delta\delta_{F,F'} = 24.0$ Hz

[g] $J(C–F) + J(C–F')$

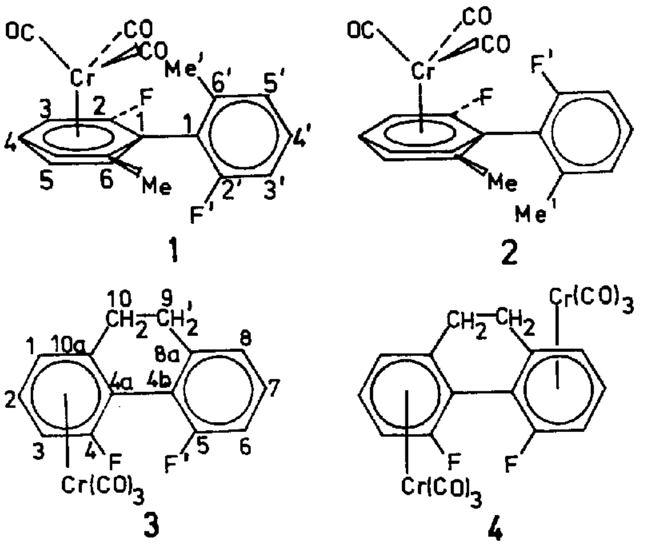

Fig. 2. Structures of complexes investigated.

mm NMR tubes. The ^{13}C NMR spectra were recorded with a Bruker AM-500 (125.76 MHz) and a Varian XL-300 (75.4 MHz). Typical acquisition and processing parameters for aromatic and (in parentheses) carbonyl regions: pulse width 60° (70°), spectral width < 100 ppm (< 1000 Hz), acquisition time 3 s (6 s), digital resolution < 0.25 points/Hz (*ca.* 0.1 points/Hz). The central line of $CDCl_3$ triplet ($\delta = 77.0$ ppm) was used as the chemical shift reference. The ^{19}F NMR spectra were recorded with a Varian XL-300 spectrometer (at 282.2 MHz). The CF_3COOH signal (0.0 ppm) was used as the external reference.

3. Results and discussion

3.1. ^{13}C NMR spectra of aromatic carbon range

The ^{13}C NMR signals in the range of aromatic carbons were assigned to the relevant carbons on the basis of their chemical shifts (Table 1), ^{13}C–^{19}F coupling constants (Table 2) and intensities. Every carbon signal was treated as a part X of the ABX spin system where A and B were fluorines. In the case of complexes **1**–**3** the chemical shift difference between fluorines, $\Delta\delta_{F,F'}$ results from the complexation of the aromatic ring and for BIP, PHE and **4** from the different isotope effect of observed ^{13}C nucleus on the chemical shift of each of fluorines. Because $\Delta\delta_{F,F'}$ values for **1**–**3** are large (see Table 3) as compared to J(C–F), the coupling constants can be measured directly from the spectrum. It is important to note that the spectral lines of the complexes are often broadened, probably because of the presence of chromium paramagnetic impurities, and therefore small splittings (< 1 Hz) may escape detection. The ratios $\Delta\delta_{F,F'}/J$(C–F) for the ligands and complex **4** are small so that determination of coupling constants requires numerical analysis of the spectrum. Every carbon of BIP with the exception of C2 gives a signal composed of six lines. Computer analysis of those signals with the LAOCOON III NMR simulation program allowed us to calculate all coupling constants and $\Delta\delta_{F,F'}$ values. The following facts prove the results obtained with this method to be reliable; (i) The J(F–F′) values, obtained from independent analyses of the signals of particular carbons, differ only slightly; (ii) The interaction of *ortho* substituents forces the aromatic rings to assume a far from planar conformation making the distance between fluorines large. The calculated J(F–F′) value is accordingly small. It cannot be excluded that the "through-bond" coupling may play a significant role here; (iii) The calculated $\Delta\delta_{F,F'}$ values, originated from differential ^{13}C isotope effects on ^{19}F chemical shifts, depend on the number of bonds separating observed carbon from both fluorines, and agree with those found for 4,4′-difluorobiphenyl [11]; (iv) When both coupled nuclei are connected with the same aromatic ring the values obtained of J(C–F) are comparable with those for the fluorobenzene derivatives. When fluorine is attached to the phenyl other than the one to which belongs the carbon observed, J(C–F) values are small and depend on the number of separating bonds. The signal of the C2 carbon of BIP is composed of the four lines. Its analysis was performed assuming $\Delta\delta_{F,F'} = 24$ Hz, the value found for carbon C2 in PHE and, following the literature [12], the negative sign of ^{1}J(C–F).

In the case of PHE and **4** only fluorine-bearing carbons give six-line signals. In analysis of those signals the values of J(F–F′) measured from ^{19}F NMR spectra were used without fitting. The spectra of the other carbons of the above compounds comprise four lines and only the sum of J(C–F) and J(C–F′) could be calculated.

3.2. ^{13}C NMR spectra of aliphatic carbon range

The spectra of the methyl carbons of BIP, as well as of the methylene carbons of PHE, comprise three lines

TABLE 3. ^{19}F NMR data

Compound	δ_F	$\delta_{F'}$	J(F–F′)
BIP		−38.7	1.4 [a]
1	−55.8	−35.9	
2	−57.9	−29.0	
PHE		−37.5	97.5 [b]
3	−52.6	−27.2	108.3 [c]
4	−49.0		112.7 [b]

[a] Mean calculated from ^{13}C NMR spectra.
[b] From ^{13}C satellites of ^{19}F NMR spectrum.
[c] From ^{19}F NMR spectrum.

and only the sum of the coupling constants of those carbons with both fluorines could be found. Each methyl group of complexes **1** and **2** gives a doublet of doublets. The coupling constants are here equal to the separations of appropriate spectral lines. It was arbitrarily assumed that for both complexes $J(C(CH_3)\text{–}F)$ and $J(C(CH_3')\text{–}F')$ are larger than $J(C(CH_3)\text{–}F')$ and $J(C(CH_3')\text{–}F)$, respectively. In the spectra of **3** two lines are observed for each CH_2 carbon. It seems reasonable to assume that this splitting originates from the "through-bond" interaction of CH_2 carbon with fluorine bonded to the same aromatic ring. Taking into account the geometries of the compounds investigated, this additional splitting, (observed for CH_3 carbons of BIP complexes but not for CH_2 carbons of **3**) could be attributed to "through-space" interaction between the nuclei involved. In the aliphatic region of the carbon spectrum of **4** one, apparently broadened, line is observed.

The following procedure was applied to interpret the spectra of **1** and **2** in the methyl carbon range. The ^1H NMR spectra of BIP, **1** and **2** were recorded and the chemical shifts of the methyl protons measured. They were 2.12 ppm for BIP, 2.04 and 2.72 ppm for **1** and 2.03 and 2.12 ppm for **2**. Then a decoupling experiment was performed in which C5′–H or C5–H signals were selectively irradiated. Inspection of the changes produced in the intensities of the methyl signals allowed us to assign the high field signals to the protons of the methyl groups bonded to the complexed aromatic ring. Such an interpretation agrees with that by Schlögl *et al.* [13] for other biphenyl derivatives. Finally, the carbon spectra of methyl groups could be identified by an off-resonance decoupling experiment. It appeared that, as in the proton case, the resonances of the carbons of the methyl groups at the complexed ring in both **1** and **2** are shifted upfield in relation to those for the ligand. This was accepted as a rule and the signals of CH_2 carbons in **3** were assigned on the basis of their chemical shifts. It is worth noting that close values of the chemical shifts of the carbons CH_2 in **3** and **4** from one side and CH_2' in **3** and PHE from the other side support that assignment.

3.3. ^{13}C *NMR spectra of carbonyl carbon range*

The chemical shifts and coupling constants of the carbonyl carbons are shown in Table 4. The spectra of **1**–**3** represent the first order pattern (doublet of doublets) where separation of the appropriate lines is equal to the relevant coupling constant. In the spectrum of **4** the triplet is observed. Such a pattern for the X part of the ABX spin system is encountered when $\Delta\delta_{AB}$ is close to zero. This is valid in the case under discussion because the isotope effect of ^{13}C nucleus of the CO group towards the chemical shifts of both fluorines is expected to be negligible. The separation of the outer lines of the triplet gives the sum of C–F and C–F′ coupling constants.

TABLE 4. ^{13}C chemical shifts (ppm) and C(O)–F coupling constants (Hz) for carbonyl carbons of investigated complexes

Complex	δ_{CO}	J(C(O)–F)	J(C(O)–F′)
1	232.20	1.9	0.0
2	231.96	2.5	5.5
3	232.15	2.0	0.8
4	231.08	2.8 [a]	

[a] J(C–F) + J(C–F′)

As mentioned above, carbonyl carbon–aromatic fluorine coupling originates mainly from "through-space" spin–spin interaction. In consequence any structural and conformational changes of the molecule, which produce a change in C(O)–F distance, will affect the coupling constant. Biphenyl derivatives appeared to be good models to illustrate such a relation. Because of the interaction of the *ortho* substituents, the rotation about the bond linking the phenyls in BIP is stopped. For this, two stable diastereomeric tricarbonylchromium complexes can be obtained. For both complexes the same number of bonds separates carbonyl carbon from fluorines but fluorine F′ and $Cr(CO)_3$ groups are placed either on the same or on the opposite sides of the plane of the complexed ring. One may expect that fluorine F′ will affect carbonyl carbon spectrum more pronouncedly in the former case. Average distance between carbonyl carbon and fluorine F, and thus the J(C(O)–F) value as well, depend on the position of the equilibrium between the rotamers $\mathbf{A} \rightleftharpoons \mathbf{B}$ (see Fig. 1). The larger the population of the conformer **A** the larger the coupling constant. Decisive for the difference in the position of the equilibrium for the discussed complexes are the steric and electronic interactions between CH_3' or F′ and CO groups. Obtained values of J(C(O)–F) and J(C(O)–F′) perfectly reflect the structural and conformational differences described above between **1** and **2**. The C–F′ coupling is absent from complex **1** in which, as found by X-ray crystallography, the $Cr(CO)_3$ moiety is located close to the CH_3' group. In **2** this coupling constant reaches the relatively large value of 5.5 Hz. The values of J(C(O)–F) are 1.9 and 2.5 Hz for **1** and **2**, respectively. Using those values the populations of the rotamer **B** were estimated in the way described previously [1]. They are 30 and 10% for **1** and **2**, respectively. This shows that the fluorine substituent of the uncomplexed ring in **2** (F′) destabilizes the rotamer **B** more efficiently than the Me′ group does in the case of **1**, probably because of its electrostatic repulsion from the CO groups. More remarks concerning the relation between molecular structure and carbonyl carbon–fluorine couplings in **2** will be presented later in this paper.

The bridge between carbons 8a and 10a in PHE increases the energy of the ground state of the rotation about the bond linking the phenyls, as compared with BIP, because the molecule is forced to assume a geometry close to that which it has in the transition state. For this reason the rotation is fast on the NMR time scale at ambient temperature ($\Delta G^{\ddagger}_{340} = 41.8$ kJ/mol [9]). It has been reported [13] that complexation reduces the barrier. Only one main product (**3**) has therefore been obtained by reaction of PHE with $Cr(CO)_6$. Its ^{13}C NMR spectrum comprises the signals which are the averages of those for the rotamers analogous to **1** and **2**. Using the terminology of Schlögl [13] they will be named *endo* and *exo*, respectively. The carbonyl carbon–fluorine coupling constants measured from the spectrum of **3** are 1.95 and 0.8 Hz. In our opinion the former value is that of the C(O)–F coupling constant because the structural difference between complexes **1** (or **2**) and **3** is not big enough to cause so dramatic a change in the equilibrium $\mathbf{A} \rightleftharpoons \mathbf{B}$, which would have the effect of lowering *J*(C(O)–F) to 0.8 Hz. Thus, the latter value is that of *J*(C(O)–F′). Having no information about populations of the *exo* and *endo* species we are not able to calculate the value of *J*(C(O)–F′) for each. The following reasoning allows us, however, to draw some rough conclusions. Because of the $-CH_2-CH_2-$ bridge the angle between the planes of the aromatic rings cannot be larger than 36° [14]. This causes the distance between CH_2' or F′ substituents and $Cr(CO)_3$ moiety to be large. In such a case one may expect that the steric interaction between those groups is weak and that none of the rotamers is pronouncedly favoured energetically. Assuming equal populations of the rotamers and neglecting the coupling in the *endo* conformer (F′ and $Cr(CO)_3$ are on the opposite sides of the complexed ring) the mean *J*(C(O)–F′) for **A** and **B** rotamers in the *exo* species may be estimated to be 1.6 Hz. When one takes into consideration the mean distances between fluorine and the $Cr(CO)_3$ group, this value, being significantly smaller than *J*(C(O)–F′) for **2** and slightly smaller than *J*(C(O)–F) for any of the investigated complexes, seems to be reasonable.

The complex **4**, with both aromatic rings complexed, was obtained as a by-product of the reaction of PHE with $Cr(CO)_6$. The data available do not allow determination of the relative configuration of $Cr(CO)_3$ moieties but on the basis of the literature [13] their location on the opposite sides of the ligand plane seems to be much more probable. As mentioned above only the sum of *J*(C(O)–F) and *J*(C(O)–F′) equal to 2.8 Hz may be obtained from the spectrum in this case. It is, however, worth noting that this is exactly equal to the sum of appropriate coupling constants for **3**. It is most likely that the *J*(C(O)–F) and *J*(C(O)–F′) couplings are the same for **4** as for **3** and this would suggest that the influence of the complexation of the second ring on the conformation of $Cr(CO)_3$ tripod and on the molecule as a whole, is small.

3.4. ^{19}F NMR spectra

In Table 3 the results of ^{19}F NMR measurements are shown. Although we are aware that the fluorine chemical shift is often related to the molecular structure in an unpredictable manner we wish to point out some interesting observations. The complexation shifts the signal of fluorine F by 11–19 ppm upfield in relation to the ligand. A similar shift was observed for the fluorobenzene complex [15]. The resonance of fluorine F′ is shifted downfield by *ca.* 3 ppm for **1** and *ca.* 10 ppm for **2** and **3**. In the former case the effect is similar to that observed for the complex of 4′-fluorobiphenyl (2.5 ppm) [15] and may be attributed to the influence of the complexation of one aromatic ring on the electronic surrounding of fluorine at the other ring. The larger shift for **2** may be connected with the direct steric interaction between $Cr(CO)_3$ and F′. It was rather a surprise to observe a large downfield shift for **3** where the mean F′–$Cr(CO)_3$ distance must be larger than in **2**. One could explain this by assuming that, in addition to the steric interaction, the electronic influence plays a more important role here than in **2** due to more effective π–π interring conjugation. In the last column of Table 3 the F–F′ coupling constants are collected. For **3** *J*(F–F′) was measured directly from the spectrum. For PHE and **4** those coupling constants were obtained from fluorine ^{13}C satellites. In this case, due to high value of the one-bond $^{13}C-^{19}F$ coupling constant (*ca.* 260 Hz) two pairs of the outermost lines of the AB part of the ABX spin system (X means ^{13}C nucleus directly bonded to F) were not overlapped by main signal of fluorine bonded to ^{12}C nucleus. The separation of the lines in each pair is equal to *J*(F–F′). For BIP the coupling constant under discussion was calculated from the numerical analysis of all aromatic carbon signals but that of C2. Unfortunately, we were not able to determine *J*(F–F′) for **1** and **2**. The NMR spectrometer available does not permit measuring proton decoupled ^{19}F NMR spectra. This, as well as line broadening originated from the paramagnetic impurities, was the reason why the lines of each part of AB spin system were not separated due to F–F′ coupling. We were able, however, to estimate those couplings to be no greater than 10 Hz. The *J*(F–F′) values obtained for investigated compounds reflect the expected distances between coupled nuclei.

4. Crystal and molecular structure of complex 1

4.1. X-Ray structure determination

A yellow, well-shaped crystal of **1** was mounted on the goniometer head of a four-circle Siemens P3 diffractometer. The crystallographic data, the parameters of data collection and refinement procedure are presented in Table 5. The crystal class, the orientation matrix and the unit cell parameters were obtained from the least-squares refinement of the angular positions measured for 25 reflections randomly selected in the 2θ range between 16 and 31. The intensities were collected up to $2\theta = 55$ (max $\sin\theta/\lambda = 0.65$) in the θ-2θ mode with the scan range 2.0° plus $K\alpha_1$–$K\alpha_2$ separation and various scan speeds between 4.2 and 29.3° min^{-1}. Two check reflections (1 2 $\bar{2}$) and (3 0 1), repeated every 70 reflections showed a decay of 1.5% and the intensities were adjusted accordingly. In total 5293 reflections were measured and corrected for the Lorentz-polarization effect. The phase problem was solved by direct methods using the SHELXS-86 program [16]. All nonhydrogen atoms were found on the most appropriate E-map. Since the absorption coefficient was comparatively high ($\mu = 7.91$ cm^{-1}) a numerical absorption correction based on a well-measured distance from a common reference point to boundary planes of the crystal was applied. The equivalent reflections were averaged. The resulting 2595 unique reflections had the internal consistency index $R_{int} = 0.012$. The structure was refined using the full-matrix least-squares technique (SHELX-76 [17]) with isotropic thermal parameters on the first step; this resulted in R equal to 0.08. The positions of the hydrogen atoms were determined on the differential Fourier-map after refinement with anisotropic thermal parameters ($R = 0.040$, unit weights). The weighting scheme with $\omega(F) = 2.550 \cdot [\sigma^2(F) + 0.000005 \cdot F_0^2]^{-1}$ gave satisfactory variance analysis. This resulted in a final value of the R factor of 0.0267 after full convergence of the refinement. A list of measured and calculated structure factors is available on request.

TABLE 5. Data collection and structure analysis parameters

Molecular formula	$CrC_{17}H_{12}O_3F_2$			
Crystal dimensions (index of limiting crystal planes and distance to common origin)	*h*	*k*	*l*	*d*(mm)
	$\bar{1}$	0	0	0.195
	1	0	0	0.195
	0	$\bar{1}$	1	0.160
	0	1	$\bar{1}$	0.160
	0	0	1	0.070
	0	0	$\bar{1}$	0.070
Space group	$P\bar{1}$			
Unit cell:				
a (Å) 7.2294(5)	$Z = 2$			
b (Å) 7.7050(8)	$M_r = 354.273$			
c (Å) 14.6342(15)	$F(000) = 360$			
α (°) 94.486(8)				
β (°) 93.404(7)				
γ (°) 114.691(7)				
V (Å³) 734.74(13)				
Density calc. (g cm^{-1})	1.602			
Linear absorption coeff. (cm^{-1})	7.91			
Radiation	graphite monochrom. Mo $K\alpha$ ($\bar{\lambda}$ 0.71069 Å)			
Temperature (K)	298			
No. reflections:				
measured	5293			
unique	2595			
unique in structure analysis ($I > 2\sigma$)	2518			
Final *R* values:				
unweighted *R*	0.0267			
weighted R_w	0.0269			
Residual extreme in final difference Fourier map (e $Å^{-3}$)	+0.24/−0.25			

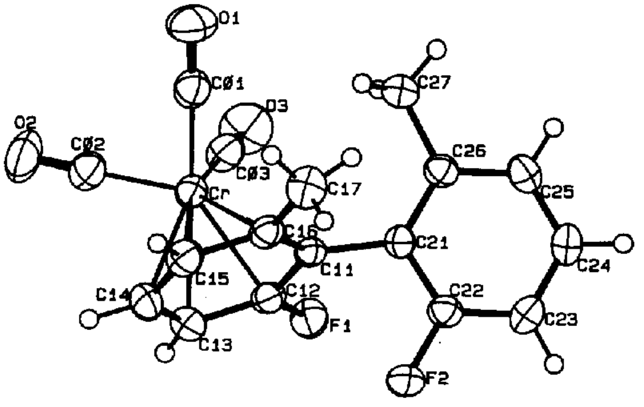

Fig. 3. X-Ray structure of 1.

4.2. *Results*

A view of the molecule (ORTEP [18]) with the atom numbering scheme is shown in Fig. 3. The final atomic coordinates and equivalent (isotropic) temperature factors with their e.s.d's for non-hydrogen atoms are listed in Table 6. Table 7 contains interatomic bond distances and Table 8 selected angles. Deviations from mean planes of aromatic rings are presented in Table 9 and selected interatomic distances shorter than 3.6 Å in Table 10. The structure obtained for complex 1 fully supports the prediction made on the basis of the carbonyl carbon–fluorine coupling constants; methyl group Me′ and $Cr(CO)_3$ are located on the same side of the

TABLE 6. Fractional atomic coordinates, equivalent temperature factors with e.s.d.'s

Atom	x	y	z	$U \times 10^4$ (Å)
CR	−0.00811(5)	0.92369(4)	0.31689(2)	316(1)
C01	0.15298(33)	0.86733(30)	0.40117(15)	417(9)
O1	0.25535(27)	0.83548(27)	0.45394(12)	642(8)
C02	0.09510(34)	1.16563(31)	0.37979(14)	442(9)
O2	0.16605(30)	1.31842(23)	0.41798(12)	677(8)
C03	0.20632(32)	1.01705(29)	0.24638(15)	422(9)
O3	0.34054(26)	1.07718(26)	0.20202(13)	680(8)
F1	−0.16738(18)	0.83929(16)	0.10056(7)	412(5)
C11	−0.20204(26)	0.64940(25)	0.22280(12)	286(7)
C12	−0.21309(27)	0.81063(26)	0.18777(12)	320(8)
C13	−0.26864(31)	0.94058(29)	0.2359(14)	377(8)
C14	−0.31564(31)	0.90958(30)	0.32687(15)	412(9)
C15	−0.30968(30)	0.75197(29)	0.36459(14)	384(8)
C16	−0.25208(27)	0.62063(26)	0.31423(13)	325(7)
C17	−0.25616(42)	0.44816(34)	0.35662(17)	448(10)
F2	−0.50643(16)	0.44215(17)	0.09345(8)	459(5)
C21	−0.17714(27)	0.50272(24)	0.15752(12)	281(7)
C22	−0.34112(27)	0.40189(26)	0.09112(13)	323(7)
C23	−0.34771(31)	0.26441(28)	0.02423(14)	382(8)
C24	−0.17991(32)	0.22402(28)	0.02243(14)	399(8)
C25	−0.01331(32)	0.31982(28)	0.08670(14)	377(8)
C26	−0.00736(27)	0.45895(26)	0.15495(13)	318(7)
C27	0.18177(37)	0.55811(39)	0.22087(19)	464(10)

TABLE 7. Bond distances (Å) in complex 1

CR–C01	1.844(3)	C11–C16	1.417(3)
CR–C02	1.835(2)	C11–C21	1.498(3)
CR–C03	1.833(2)	C12–C13	1.385(3)
CR–C11	2.273(2)	C13–C14	1.407(3)
CR–C12	2.204(2)	C14–C15	1.388(4)
CR–C13	2.221(2)	C15–C16	1.417(3)
CR–C14	2.194(2)	C16–C17	1.500(4)
CR–C15	2.215(2)	F2–C22	1.356(3)
CR–C16	2.259(2)	C21–C22	1.389(2)
C01–O1	1.148(3)	C21–C26	1.404(3)
C02–O2	1.149(3)	C22–C23	1.369(3)
C03–O3	1.151(3)	C23–C24	1.374(4)
F1–C12	1.349(2)	C24–C25	1.376(3)
C11–C12	1.411(3)	C25–C26	1.392(3)
		C26–C27	1.496(3)

TABLE 8. Selected bond angles (deg.)

C15–CR–C16	36.96(07)	C14–C15–C16	121.58(19)
C14–CR–C15	36.70(08)	C15–C16–C17	119.56(18)
C13–CR–C14	37.17(08)	C11–C16–C17	121.09(18)
C12–CR–C13	36.49(08)	C11–C21–C26	127.64(17)
C11–CR–C12	36.69(07)	C11–C21–C22	115.36(18)
C02–CR–C03	87.00(10)	C22–C21–C26	116.99(17)
C01–CR–C03	89.92(11)	F2–C22–C21	117.43(17)
C01–CR–C02	87.35(10)	C21–C22–C23	124.59(20)
C16–C11–C21	123.78(16)	F2–C22–C23	117.98(18)
C12–C11–C21	118.59(16)	C22–C23–C24	117.66(19)
C12–C11–C16	116.62(17)	C23–C24–C25	120.08(20)
F1–C12–C11	117.37(16)	C24–C25–C26	122.15(22)
C11–C12–C13	124.95(17)	C21–C26–C25	118.52(19)
F1–C12–C13	117.68(16)	C25–C26–C27	118.42(20)
C12–C13–C14	117.22(19)	C21–C26–C27	123.05(19)
C13–C14–C15	120.34(20)		

TABLE 9. Deviations (Å) of atoms from least-squares planes of aromatic rings of 1. Asterisked carbons were used for definition of plane

Uncomplexed ring $0.1528 \times x + 0.7787 \times y - 0.6085 \times z = 0.6811$		Complexed ring $-0.7826 \times x - 0.5197 \times y - 0.3429 \times z = -0.3471$	
Atom	Deviation	Atom	
C21*	0.0010(17)	C11*	−0.0018(20)
C22*	0.0008(19)	C12*	0.0006(20)
C23*	−0.0023(20)	C13*	0.0041(23)
C24*	0.0012(20)	C14*	−0.0077(24)
C25*	0.0012(20)	C15*	0.0054(23)
C26*	−0.0022(19)	C16*	−0.0005(20)
C27	0.0225(28)	C17	0.0700(30)
F2	−0.0060(12)	F1	0.0094(13)
C11	0.0315(18)	C21	0.2456(20)
		Cr	−1.7290(5)

complexed ring. The $Cr(CO)_3$ tripod is rotated about 10° from *eclipsed* conformation of appropriate Cr–CO and C16–CH_3, C14–H or C12–F1 bonds. It agrees with the high population of rotamer **A** (70%) estimated for this complex. The carbon of uncomplexed ring do not deviate significantly from planarity. On the contrary such a deviation is observed for the carbons of the other ring. The bond C14–Cr is shortest of those between chromium and aromatic carbons and, at the same time, carbon C14 deviates most from the mean aromatic ring plane towards chromium. Neighbouring carbons C13 and C15 are displaced from that plane in the opposite direction. The averaged length of the aromatic carbon–carbon bond in complexed ring (1.384 Å) is shorter than that in uncomplexed ring (1.404 Å). The dihedral angle formed by the mean planes of aromatic rings is 108.4°. The distances of the carbon of methyl group C27 to the closest carbonyl carbons, C01 and C03, differ slightly and are 3.490 and 3.455 Å, respectively. Bond angles F1–C12–C11 (117.4°) and C12–C11–C21 (118.6°) are smaller than angles C17–C16–C11 (121.1°) and C16–C11–C21 (123.0°), respectively. The same relation is maintained in the uncomplexed ring but angles C27–C26–C21 (223.0°) and C26–C21–C11 (127.6°) are larger and angle C22–C21–C11 (115.4°) smaller than appropriate angles in complexed ring. This might be caused by repulsion between $C(27)H_3$ and $Cr(CO)_3$ groups. Finally, the short intermolecular distance of 2.397 Å between F2 and F2 $(-x-1, -y+1, -z)$ atoms is worth noticing.

We were interested to find out if the observed J(C(O)–F) and J(C(O)–F′) values in complex **2** correspond to separations between appropriate nuclei. Having no crystallographic data for **2** accessible at this moment we decided to use those for **1** assuming that, with exception of the torsional angle defined by atoms C22, C21, C11 and C12, other geometrical parameters differ too little to affect the results of our rough, qualitative consideration. In a computer simulated structure of **2** obtained from **1** by the rotation of the uncomplexed aromatic ring 180° about C11–C22 bond, the distances between carbons C01 and C03 and fluorine F2 are 2.934 and 3.026 Å, respectively. The distance C03–F1 is 3.081 Å. It should now be recalled which factors affect observed coupling constants. J(C(CO)–F) value depends on the value of the coupling constant for $Cr(^{13}CO)(^{12}CO)_2$ conformer in which Cr–^{13}CO and C_{Ar}–F bonds are *eclipsed* (in any other conformer this coupling is absent) and on its population equal to one third of the total population of rotamer **A** (see Fig. 4). The C(O)–F′ interactions, which affect J(C(O)–F′), may be effective in two of three conformers of **A** type. Taking into account appropriate internuclear distances, the coupling constants J(C(O)–F′) for each of those conformers should not be smaller than J(C(O)–F). Moreover, one must not forget the C(O)–F′ interaction in one of three conformers of type **B**. This interaction, though less populated, may play an important role because the C(O)–F′ distance is expected to be significantly short. The above consideration predicts J(C(O)–F′) to be at least twice J(C(O)–F), and this agrees with what is observed.

TABLE 10. Selected interatomic contacts shorter than 3.6 Å.

Cr ··· F1	3.2234(11)	C03 ··· C12	2.8121(26)
C01 ··· C02	2.5409(38)	C03 ··· C27	3.4549(40)
C01 ··· C03	2.5984(32)	F1 ··· F2	3.0060(14)
C01 ··· C27	3.4897(38)	C11 ··· F2	2.6594(18)
C02 ··· C03	2.5248(34)	C11 ··· C27	3.1355(38)
C02 ··· C14	2.8112(27)	C12 ··· F2	2.9107(19)
C03 ··· F1	3.0814(23)	C16 ··· F2	3.4926(21)

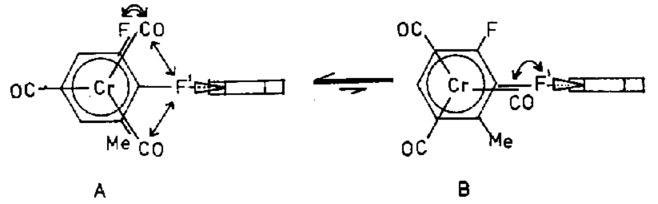

Fig. 4. ^{13}C–^{19}F coupling affecting carbonyl carbon–fluorine F (⇔) and–fluorine F′ (↔) interactions in complex **2**.

5. Perspectives

Finally, we wish to report out attempts to extend the investigation of carbonyl carbon–fluorine coupling to other classes of carbonylchromium complexes. We planned to include the complex of 4,5-difluorophenanthrene in the series presented in this work. This must, however, be postponed because the ligand is not yet prepared in an amount sufficient for its complexation. The tricarbonylchromium complex of 3-(trifluoromethyl)anisole was investigated in the hope of observing C(O)–F coupling with fluorine attached to sp^3 hybridized benzylic carbon. We found this coupling absent unless it is in fact really small. The quality of the sample was good so it was possible to record a well resolved proton coupled spectrum of carbonyl carbons (pentet, J(C(O)–H) = 0.7 Hz). When protons were decoupled the singlet with 0.6 Hz half-height width was observed instead. The answer to the question whether the distance between nuclei is too large or whether the coupling demands fluorine to be bonded to sp^2 hybridized carbon, needs more experimental data. The series of phosphinedicarbonylchromium complexes of fluorobenzene derivatives has been prepared and their

^{13}C NMR spectra interpreted with respect to the conformation of the complexing group. The results will soon be published.

Recently, investigations of pentacarbonylchromium complexes have been undertaken. The carbon–fluorine coupling constants for the complex of 2-fluoropyridine were found to be 7.6 and 1.7 Hz for *cis* and *trans* carbonyls, respectively. The attempt to prepare the complex of 8-fluorochinoline failed because of its extreme sensitivity to air, light and temperature even in solid state. Further investigations on that subject are planned.

Acknowledgments

We express our appreciation to the State Committee of Scientific Research for supporting this work within the PB 185/2/91 project, and to Professor J. Dabrowski of Max Planck Institut für Medizinische Forschung, Heidelberg, for the use of the 500 MHz spectrometer.

References

1 P. Szczeciński, *J. Organomet. Chem., 423* (1992) 23.
2 P. Szczeciński, *J. Organomet. Chem., 393* (1990) 111.
3 P. Szczeciński and K. Wisniewski, *J. Organomet. Chem., 423* (1992) C13.
4 G. W. Gribble and W.J. Kelly, *Tetrahedron Lett., 26* (1985) 3779.
5 F. R. Jerome and K. L. Servis, *J. Am. Chem. Soc., 94* (1972) 5896.
6 L. C. Hsee and D. J. Sardella, *Magn. Reson. Chem., 28* (1990) 688.
7 I. D. Rae, A. Staffa, A. C. Diz, C. G. Giribet, M. C. Ruiz de Azua and R. H. Contreras, *Aust. J. Chem., 40* (1987) 1923.
8 S. R. Ahmed and D. M. Hall, *J. Chem. Soc.*, (1958) 3043.
9 R. Cosmo and S. Sternhell, *Aust. J. Chem., 40* (1987) 35.
10 C. A. L. Mahaffy and P. L. Pauson, *Inorg. Synth., 19* (1979) 154.
11 T. Schaeffer, J. Peeling and G. H. Penner, *Can. J. Chem., 64* (1986) 2162.
12 S. L. Manatt, M. A. Cooper, C. W. Mallory and F. B. Mallory, *J. Am. Chem. Soc., 95* (1973) 975.
13 H. Kalchhauser, K. Schlögl, W. Weissensteiner and A. Werner, *J. Chem. Soc., Perkin Trans. I*, (1983) 1723.
14 R. Cosmo, T. W. Hambley and S. Sternhell, *J. Org. Chem., 52* (1987) 3119.
15 V. S. Khandkarova, S. P. Gupin and B. A. Kvasov, *J. Organomet. Chem., 23* (1970) 509.
16 G. M. Sheldrick, *SHELXS-86, Program for Crystal Structure Determination*, University of Göttingen, Germany, 1986.
17 G. M. Sheldrick, *SHELX-76, Program for Crystal Structure Determination*, University of Cambridge, Cambridge, UK, 1976.
18 C. K. Johnson, *ORTEP Report ORNL-5183*, Oak Ridge National Laboratory, Oak Ridge, TN, 1976.